Supplementary Information

N-Functionalisation of 5,5'-bistetrazole providing 2,2'-di(azidomethyl)bistetrazole: A melt-castable metal-free green primary explosive

Thomas M. Klapötke*, Moritz Kofen, and Jörg Stierstorfer

Department of Chemistry, Ludwig-Maximilian University of Munich,

Butenandtstr. 5-13, D-81377 Munich, Germany.

tmk@cup.uni-muenchen.de, FAX +49 89 2180 77492

Table of Contents

1. Experimental part and general methods

All chemicals and solvents were employed as received (Sigma-Aldrich, Fluka, Acros, ABCR). ^{1}H, $^{13}C\{^{1}H\}$, ^{14}N, and $^{15}N\{^{1}H\}$ spectra were recorded at ambient temperature using a JEOL Bruker 27400, Eclipse 270, JEOL EX 400 or a JEOL Eclipse 400 instrument. The chemical shifts quoted in ppm in the text refer to typical standards such as tetramethylsilane (^{1}H, ^{13}C) nitromethane (^{14}N,^{15}N) in DMSO-d_6, D_20 or acetone-d_6 as the solvent. Endothermic and exothermic events of the described compounds, which indicate melting, loss of crystal water or decomposition, are given as the extrapolated onset temperatures. The samples were measured in a range of 25–400 °C at a heating rate of 5 °C min^{-1} through differential thermal analysis (DTA) with an OZM Research DTA 552-Ex instrument and in some cases additionally by thermal gravimetric analysis (TGA) with a PerkinElmer TGA4000. Infrared spectra were measured with pure samples on a Perkin-Elmer BXII FT-IR system with a Smith DuraSampler IR II diamond ATR. Determination of the carbon, hydrogen, and nitrogen contents was carried out by combustion analysis using an Elementar Vario El (nitrogen values determined are often lower than the calculated ones' due to their explosive behavior). Impact sensitivity tests were carried out according to STANAG 4489[S1] with a modified instruction[S2] using a BAM (Bundesanstalt für Materialforschung) drophammer.[S3] Friction sensitivity tests were carried out according to STANAG 4487[S4] with a modified instruction[S5] using the BAM friction tester.[S6,7] The classification of the tested compounds results from the "UN Recommendations on the Transport of Dangerous Goods".[S8, 9] Additionally, all compounds were tested upon the sensitivity toward electrical discharge using the OZM Electric Spark XSpark10 device.[S7] Energetic properties have been calculated with the EXPLO5 6.05.04 computer code[S10] using the, X-ray densities, recalculated to room temperature by applying the equation for volumetric expansion[S31] and calculated solid state heats of formation. These were computed by the atomization method as described in recently published papers. Electronic enthalpies were calculated with the Gaussian09 software[S11] suite using the CBS-4M method. Hot plate and hot needle tests were performed in order to classify the initiation capability of compound **3**. **3** was fixed on a copper plate underneath adhesive tape and initiated by a red-hot needle. Strong deflagration or detonation of the compound usually indicates a valuable primary explosive. The safe and straightforward hot plate test only shows the behavior of the unconfined sample toward fast heating on a copper plate. It does not necessarily allow any conclusions on a compound´s capability as a suitable primary explosive. Initiation capability tests of the newly synthesized compound **3** towards pentaerythritol tetranitrate (PETN) was carried out in a cooper shell with a diameter of 7 mm and a length of 88 mm filled with 200 mg of sieved PETN (grain size < 100 µm). First, nitropenta was pressed with a weight of 8 kg, then the primary explosive **3** was subsequently filled on top of the main charge. The shell was sealed by an insulator, placed in a retaining ring, which was soldered to a copper witness plate with a thickness of 1 mm and finally initiated by a type A electric igniter. A positive test is indicated by a hole in the copper plate and fragmentation of the shell caused by a deflagration-to-detonation transition (DDT) of PETN.

1.1 1,1'-, 1,2-, 2,2'-di(hydroxymethyl)bistetrazole (1a, b, c)

Ammonium bistetrazolate (15 g, 87 mmol) was dissolved in water (92.4 mL), formaldehyde (37%, 36 mL, 484 mmol, 5.6 eq.) and HCl (37%, 19.5 mL, 235.5 mmol, 2.7 eq.) was added, and the mixture was heated overnight at 60 °C. After cooling down, the solution was extracted into ethyl acetate (500 mL), cleared from water with $MgSO_4$ and dried *in vacuo*, resulting in a mixture of 1,1'- (**1a**), 1,2- (**1b**), and 2,2'-di(hydroxymethyl)bistetrazole (**2c**) as a white solid (15.66 g, 79 mmol, 90%).

^{1}H NMR (acetone-d_6, ppm) δ = 6.34 (s, 4H, 2 CH_2), 6.25 (s, 2H, CH_2), 6.21 (s, 2H, CH_2), 6.19 (s, 4H, 2 CH_2); **^{13}C NMR** (DMSO-d_6, ppm) δ = 155.4 (2 N_4C), 75.9 (2 CH$_2$).

1.2 2,2'-di(chloromethyl)bistetrazole (2)

The isomeric mixture of 1a, b and c (2.5 g, 13 mmol) was suspended in dichloromethane (50 mL). $SOCl_2$ (2 mL, 28 mmol, 2.2 eq.), followed by pyridine (3 mL, 39 mmol, 3.0 eq.) was added and the reaction stirred for 30 min at temperatures below 10 °C and was then allowed to warm to room temperature over 2.5 h. The DCM-phase was then washed with water, HCl (2 M) and again water. The solvent was dried with $MgSO_4$ and removed *in vacuo*, resulting in 2,2'-di(chloromethyl)-bistetrazole (**2**) as an off-white powder in good yield (2.49 g, 11 mmol, 84%).

^{1}H NMR (acetone-d_6, ppm) δ = 6.78 (s, 4H, 2 CH_2); **^{13}C NMR** (acetone-d_6, ppm) δ = 157.2 (2 N_4C), 57.6 (2 *C*H_2).

1.3 2,2'-di(azidomethyl)bistetrazole (3)

Crude 2,2'-di(chloromethyl)-bistetrazole (**2**) (200 mg, 0.85 mmol) and NaN_3 (331 mg, 5.11 mmol, 6 eq.) were added to a mixture of water and acetone (12 mL, 1:3) and refluxed at 75°C overnight. The product was extracted into dichloromethane (3x20 mL), washed with BRINE and dried over $MgSO_4$. After removing the solvent *in vacuo*, 2,2'-di(azidomethyl)bistetrazole (**3**) is obtained as colorless solid in good yield (196 mg, 0.79 mmol, 93%)

^{1}H NMR (DMSO-d_6, ppm) δ = 6.39 (s, 4H, 2 CH_2); **^{13}C NMR** (DMSO-d_6, ppm) δ = 155.6 (2 N_4*C*), 65.7 (2 *C*H_2); **^{15}N{1H} NMR** (DMSO-d_6, ppm) δ = 3.0 (s, N3/3'), −46.9 (s, N4/4'), −76.8 - −76.9 (t, N1/1') , −90.6 (s, N2/2') , −135.9 - −136.2 (t, N8/8') , −159.6 (s, N9/9'), −302.1 (s, N7/7'). **Elemental analysis** calcd. [%] for $C_4H_4N_{14}$ (248.17): C 19.36, H 1.62, N 79.02; found C 20.28, H 1.99, N 79.25; **IR**: (ATR, cm^{-1}): ṽ = 3047 (w), 2991 (w), 2167 (m), 2148 (m), 2126 (s), 2102 (vs), 1450 (w), 1440 (w), 1398 (m), 1364 (vw), 1338 (m), 1325 (m), 1253 (vs), 1237 (vs), 1201 (vs), 1165 (m), 1054 (s), 1010 (s), 917 (vs), 755 (vs), 728 (s), 684 (s), 655 (s), 558 (m), 413 (s); **DTA** (5 °C min^{-1})**:** 102 °C (T_{endo}), 177 °C (T_{exo}); **BAM drophammer**: 2 J, **BAM friction tester**: <0.1 N.

1.4 2,2'-di(nitratomethyl)bistetrazole (4)

Crude mixture of 2,2'-di(hydroxymethyl)bistetrazole (2 g, 10 mmol) was added to a fresh mixture of HNO_3 (2 mL, 48 mmol, 4.8 eq.) and acetic anhydride (6 mL, 63 mmol, 6.3 eq.) at temperatures below 10 °C. The mixture was then stirred for 4 h at temperatures between 0-10 °C, quenched on ice-water (50 mL) and stirred for 2 h. The precipitate is filtered off and purified by column chromatography with DCM, to obtain 2,2'-di(nitratomethyl)bistetrazole (**4**) as a white solid in moderate yield (44%).

^{1}H NMR (acetone-d_6, ppm) δ = 7.29 (s, 4H, 2 CH_2); **^{13}C NMR** (acetone-d_6, ppm) δ = 157.1 (2 N_4*C*), 78.4 (2 *C*H_2); **Elemental analysis** calcd. [%] for $C_4H_4N_{10}O_6$ (288.14): C 16.67, H 1.40, N 48.61; found: C 17.02, H 1.89, N 49.16; **IR**: (ATR, cm^{-1}): ṽ = 3051 (w), 2994 (vw), 2958 (vw), 2923 (vw), 2853 (vw), 1711 (m), 1671 (vs), 1421 (m), 1404 (m), 1391 (m), 1349 (m), 1323 (w), 1284 (vs), 1253 (m), 1218 (m), 1178 (m), 1051 (m), 1030 (s), 1002 (m), 969 (s), 826 (vs), 772 (vs), 742 (s), 731 (s), 696 (w), 680 (s), 632 (vs), 573 (s), 409 (s); **DTA** (5 °C min^{-1})**:** 100 °C (T_{endo}), 152 °C (T_{exo}); **BAM drophammer**: <1 J, **BAM friction tester**: 0.3 N.

2 Crystallographic data

For all crystalline compounds, an Oxford Xcalibur3 diffractometer with a CCD area detector or Bruker D8 Venture TXS diffractometer equipped with a multilayer monochromator, a Photon 2 detector and a rotating-anode generator were employed for data collection using Mo-K_α radiation (λ = 0.7107 Å). On the Oxford device, data collection and reduction were carried out using the CrysAlisPRO software.[S13] On the Bruker diffractometer, the data were collected with the Bruker Instrument Service v3.0.21, the data reduction was performed using the SAINT V8.18C software (Bruker AXS Inc., 2011). The structures were solved by direct methods (SIR-92,[S14] SIR-97,[S15,16] SHELXS-97[S17,18] or SHELXT[S19]) and refined by full-matrix least-squares on *F*2 (SHELXL[S17,18])

and finally checked using the PLATON software[S20] integrated in the WinGX[S19,21] or Olex2[S20] software suite. The non-hydrogen atoms were refined anisotropically and the hydrogen atoms were located and freely refined. The absorptions were corrected by a SCALE3 ABSPACK or SADABS Bruker APEX3 multi-scan method.[S22,23] All DIAMOND2 plots are shown with thermal ellipsoids at the 50% probability level and hydrogen atoms are shown as small spheres of arbitrary radius.

Table S1. Crystallographic data and structure refinement details for compounds **1c** and **2**

	1c	**2**
Formula	$C_4H_6N_8O_2$	$C_4H_4Cl_2N_8$
FW [g mol^{-1}]	198.17	235.05
Crystal system	monoclinic	monoclinic
Space group	$P2_1/n$ (No. 14)	$P2_1/c$ (No. 14)
Color / Habit	colorless block	colorless platelet
Size [mm]	0.14 x 0.17 x 0.39	0.02 x 0.06 x 0.10
a [Å]	4.5207(5)	8.3693(4)
b [Å]	7.9263(9)	8.2279(4)
c [Å]	11.5245(12)	6.7862(3)
α [°]	90	90
β [°]	98.503(10)	108.194(2)
γ [°]	90	90
V [Å^3]	408.41(8)	443.95(4)
Z	2	2
$\rho_{calc.}$ [g cm^{-3}]	1.612	1.758
μ [mm^{-1}]	0.133	0.703
F(000)	204	236
$\lambda_{MoK\alpha}$ [Å]	0.71073	0.71073
T [K]	107	105
θ Min-Max [°]	3.1, 26.4	3.6, 30.5
Dataset	−5: 5; −9: 9; −14: 14	−11: 11; −11: 11; −9: 9
Reflections collected	3697	11605
Independent refl.	834	1355
R_{int}	0.024	0.033
Observed reflections	727	1190
Parameters	76	72
R_1 (obs)[a]	0.0313	0.0273
wR_2 (all data)[b]	0.0811	0.0683
S[c]	1.05	1.11
Resd. Dens [e Å^{-3}]	−0.17, 0.24	−0.30, 0.41

Device type	Oxford Xcalibur3	Oxford Xcalibur3
Solution	SIR−92	SIR-92
Refinement	SHELXL-2018	SHELXL-2018
Absorption correction	multi-scan	multi-scan

[a] $R_1 = \Sigma||F_0|-|F_c||/\Sigma|F_0|$; [b] $wR_2 = [\Sigma[w(F_0^2-F_c^2)^2]/\Sigma[w(F_0)^2]]^{1/2}$; $w = [\sigma c^2(F_0^2)+(xP)^2+yP]^{-1}$ and $P=(F_0^2+2F_c^2)/3$; [c] $S = \{\Sigma[w(F_o^2-F_c^2)^2]/(n-p)\}^{1/2}$ (n = number of reflections; p = total number of parameters).

Table S1. Crystallographic data and structure refinement details for compounds **3** and **4**

	3	**4**
Formula	$C_4H_4N_{14}$	$C_4H_4N_{10}O_6$
FW [g mol^{-1}]	248.21	288.17
Crystal system	tetragonal	tetragonal
Space group	$I4_1/a$ (No. 88)	$P\bar{4}2_1c$ (No.114)
Color / Habit	colorless platelet	colorless block
Size [mm]	0.06 x 0.15 x 0.38	0.32 x 0.46 x 0.51
a [Å]	17.1656(10)	9.4429(1)
b [Å]	17.1656(10)	9.4429(1)
c [Å]	6.7040(7)	12.3008(3)
α [°]	90	90
β [°]	90	90
γ [°]	90	90
V [Å^3]	1975.4(3)	1096.84(4)
Z	8	4
$\rho_{calc.}$ [g cm^{-3}]	1.669	1.745
μ [mm^{-1}]	0.131	0.160
F(000)	1008	584
$\lambda_{MoK\alpha}$ [Å]	0.71073	0.71073
T [K]	113	108
θ Min-Max [°]	2.4, 26.4	2.7, 32.8
Dataset	−21: 20 ; −20: 21 ; −8: 8	−14: 14 ; −13: 13 ; −18: 18
Reflections collected	6544	22865
Independent refl.	1009	1950
R_{int}	0.073	0.040
Observed reflections	698	1764
Parameters	90	99
R_1 (obs)[a]	0.0441	0.0304
wR_2 (all data)[b]	0.0976	0.0810
S [c]	1.03	1.07
Resd. dens [e Å^{-3}]	−0.20, 0.18	−0.14, 0.29
Device type	Oxford Xcalibur3	Oxford Xcalibur3
Solution	SIR-92	SIR-92
Refinement	SHELXL-2018	SHELXL-2018
Absorption correction	multi-scan	multi-scan

[a] $R_1 = \Sigma||F_0|-|F_c||/\Sigma|F_0|$; [b] $wR_2 = [\Sigma[w(F_0^2-F_c^2)^2]/\Sigma[w(F_0)^2]]^{1/2}$; $w = [\sigma c^2(F_0^2)+(xP)^2+yP]^{-1}$ and $P=(F_0^2+2F_c^2)/3$; [c] $S = \{\Sigma[w(F_o^2-F_c^2)^2]/(n-p)\}^{1/2}$ (n = number of reflections; p = total number of parameters).

2.1 Crystal structures of 1c and 2

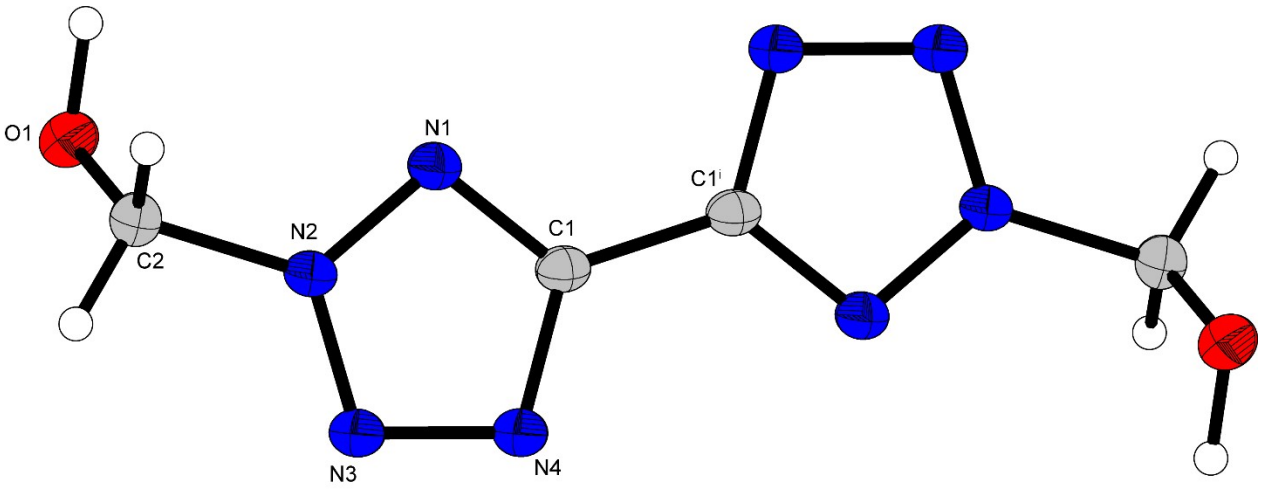

Figure S1. Crystal structure of compound **1c**; Selected interatomic distances [Å]: O1-C2 1.3854(17), N3-N4 1.3263(17), N1-N2 1.3309(15), N4-C1 1.3520(18), N1-C1 1.3228(17), C1-C1_a 1.4580(18), O1-H1 0.95(2), C2-H2A 0.969(16), N2-N3 1.3207(16), C2-H2B 0.978(15), N2-C2 1.4855(18); Angles [°]: N2-N1-C1 101.35(10), N4-C1-C1^{i} 123.41(11), C2-O1-H1 104.4(14), N1-C1-C1^{i} 123.58(12), N1-N2-N3 114.11(11), O1-C2-N2 110.01(11), N1-N2-C2 122.83(11), N3-N2-C2 123.06(11), N2-N3-N4 105.99(11), N3-N4-C1 105.55(11), N1-C1-N4 113.00(11).

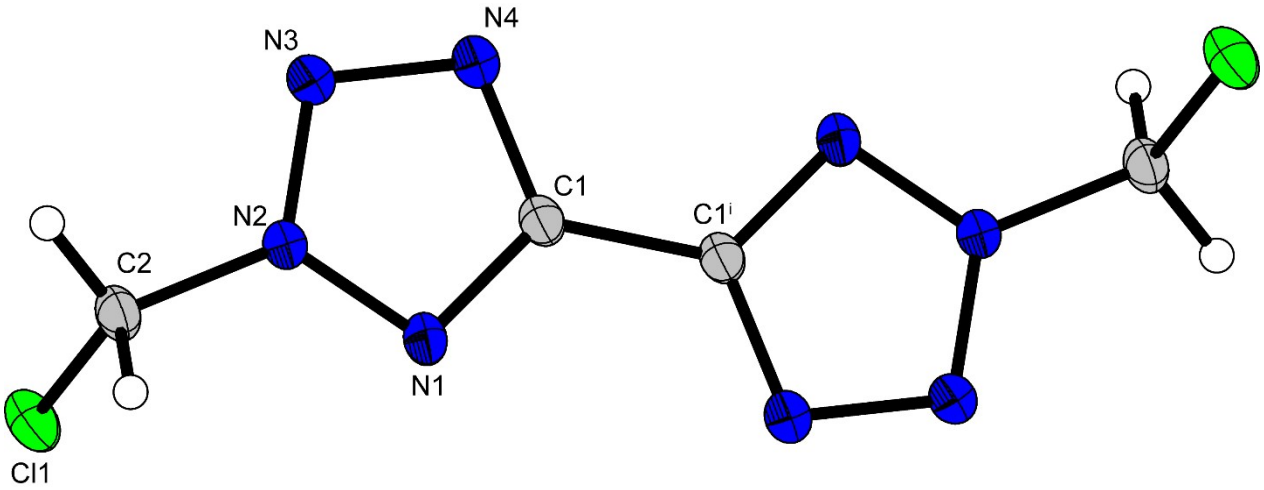

Figure S2. Crystal structure of compound **2**; Selected interatomic distances [Å]: C1-C1^{i} 1.4568(19), N1-C1 1.3288(17), N1-N2 1.3285(17), N2-N3 1.3279(15), N2-C2 1.4480(17), N3-N4 1.3158(17), N4-C1 1.3549(17), Cl1-C2 1.7737(14); Angles [°]: N2-N1-C1 100.81(10), N4-C1-C1^{i} 123.51(11), N1-N2-N3 114.35(11), Cl1-C2-N2 111.41(9), N1-N2-C2 123.43(11) , N3-N2-C2 122.20(11) , N2-N3-N4 106.06(11), N3-N4-C1 105.59(11), N1-C1-N4 113.19(12), N1-C1-C1^{i} 123.30(12).

The bond angles and distances in compound **1c**-**4** are in the typical range for N–N, C–N, and N–O single bonds, as well as N–N and C–N double bonds. Compounds **1c** and **2** both show perfectly planar bistetrazole scaffolds with torsion angles between N1-C1-C1^{i}-N1^{i} of 180 ° (**1c**) and 179.98 (**2**). Also, the methylene groups are protruding from the bistetrazole plane in opposite directions for both compounds, too.

3. Computations

All calculations were carried out using the Gaussian G09 program package.[S11] The enthalpies (H) and free energies (G) were calculated using the complete basis set (CBS) method of Petersson and coworkers in order to obtain very accurate energies.[S12] The CBS models use the known asymptotic convergence of pair natural orbital expressions to extrapolate from calculations using a finite basis set to the estimated complete basis set limit. CBS-4 begins with a HF/3-21G(d) geometry optimization; the zero point energy is computed at the same level. It then uses a large basis set SCF calculation as a base energy, and a MP2/6-31+G calculation with a CBS extrapolation to correct the energy through second order. A MP4(SDQ)/6-31+(d,p) calculation is used to approximate higher order contributions. In this study we applied the modified CBS-4M method (M referring to the use of minimal population localization) which is a re-parametrized version of the original CBS-4 method and also includes some additional empirical corrections. The enthalpies of the gas-phase species M were computed according to the atomization energy method (E1) (Table S3 & 4).[S11,13,24-27]

$$\Delta_f H^\circ_{(g,\,M,\,298)} = H_{(Molecule,\,298)} - \sum H^\circ_{(Atoms,\,298)} + \sum \Delta_f H^\circ_{(Atoms,\,298)} \qquad (E1)$$

Table S3. Literature values for atomic $\Delta H^\circ_f{}^{298}$ / kcal mol^{-1}

	$-H^{298}$ [a.u.]	NIST[S28]
H	0.50091	52.1
C	37.786156	171.3
N	54.522462	113.0
O	74.991202	59.6

The gas-phase heat of formations were converted to the solid/liquid state ones for neutrals: by subtracting the vaporization/sublimation enthalpies (calculated using the Trouton rule)[S29,30] At last, the molar standart enthalpies of formation ($\Delta_f H_M$) were used to calculate the molar solid state energie of formation (ΔU_m) according to equation (E2), Δn being the change of moles of gaseous components. The calculation results are summarized in Table S7.

$$\Delta U_m = \Delta H_m - \Delta n\, R\, T \qquad \text{(E2)}$$

Table S4. CBS-4M results, Gas phase enthalpies of formation, calculated sublimation/vaporization enthalpies and solid-state heat of formation.

Compound	$-H^{298}$ / a.u.	$\Delta_f H°$(g) / kJ mol^{-1}	$\Delta H°_{sub}$ / kJ mol^{-1}	Δn
3	–919.901609	1328.3	1258.0	–9
4	–1151.921856	505.0	440.5	–10

4. NMR spectroscopy of 1c-4

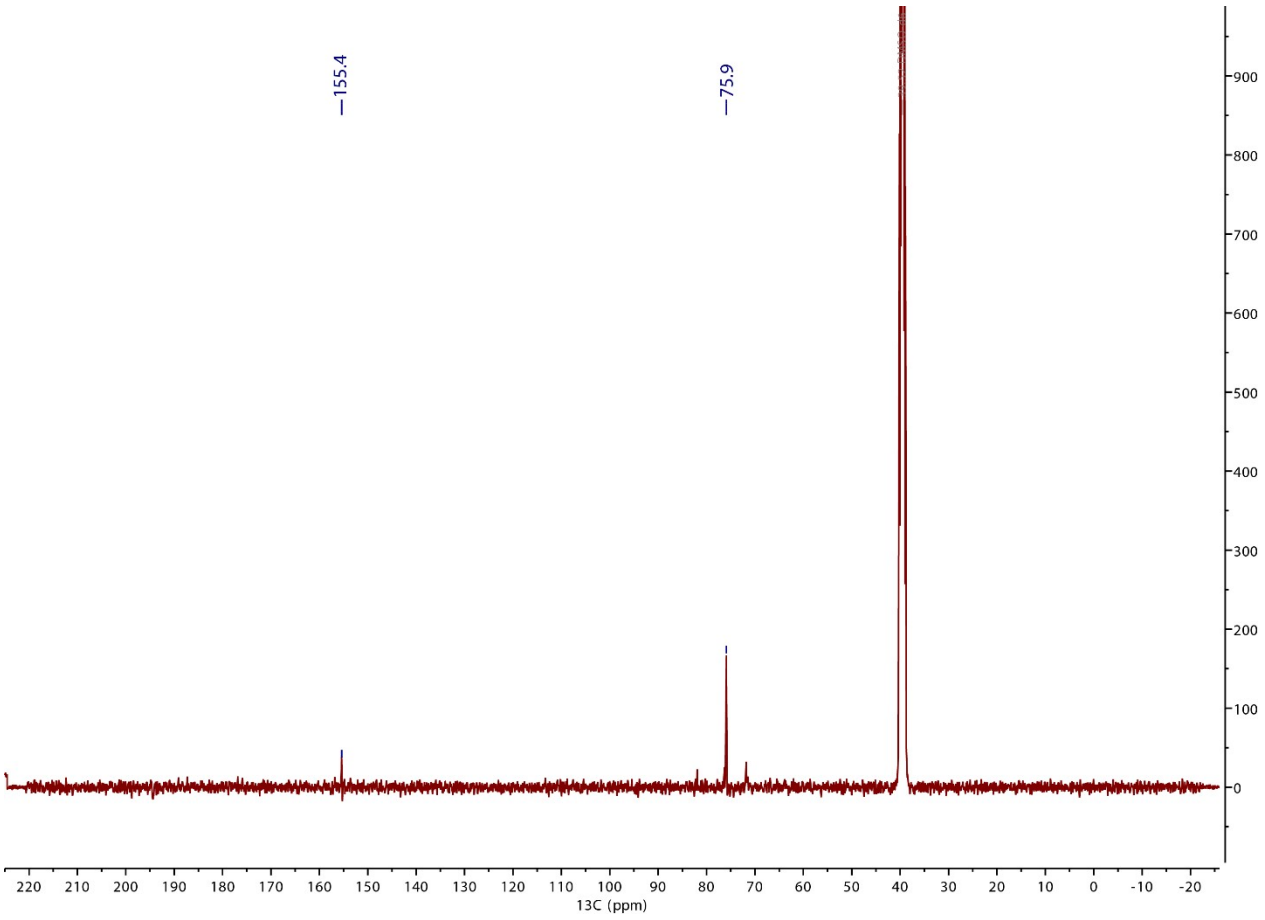

Figure S3. $^{13}C\{^{1}H\}$ NMR of **1c** in DMSO-d_6.

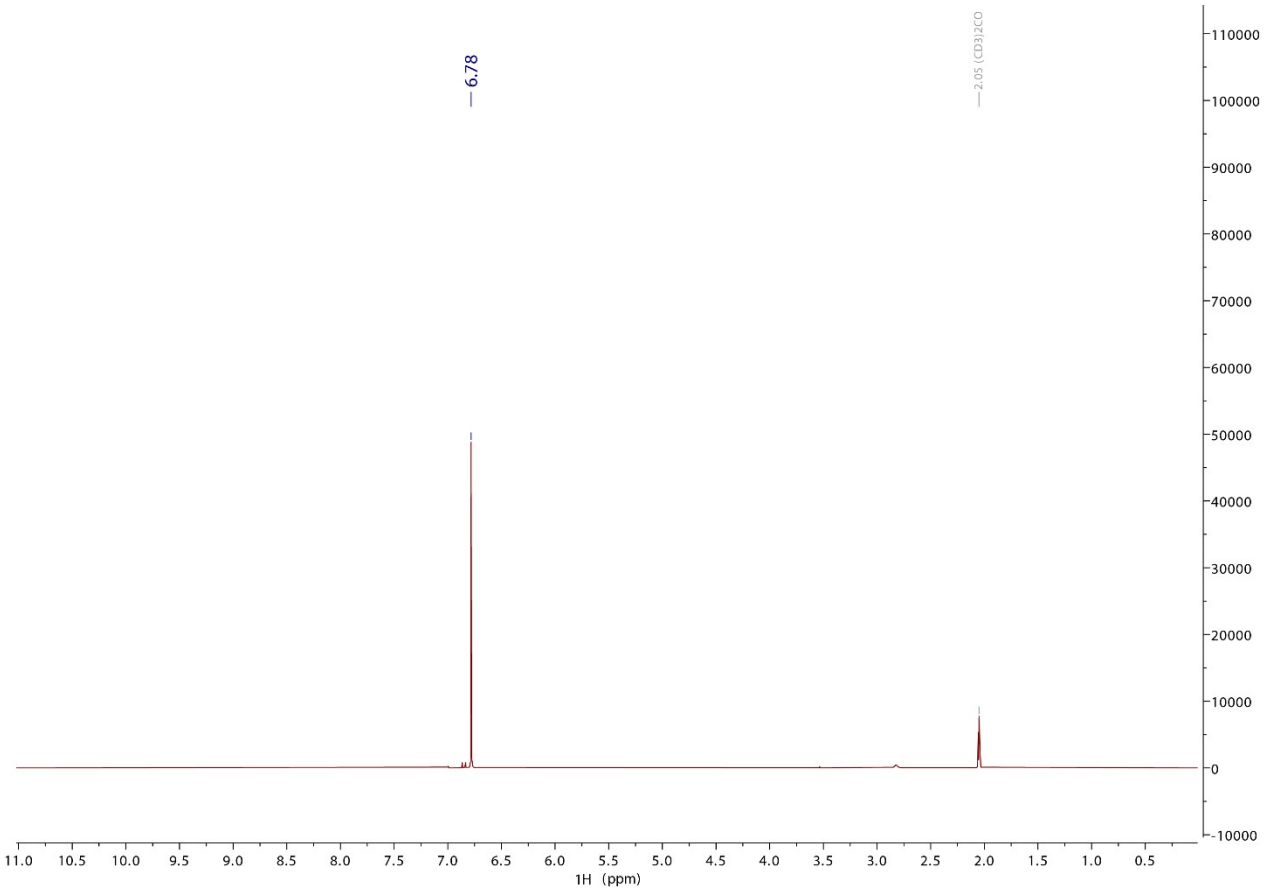

Figure S4. ^{1}H NMR of **2** in acetone-d_6.

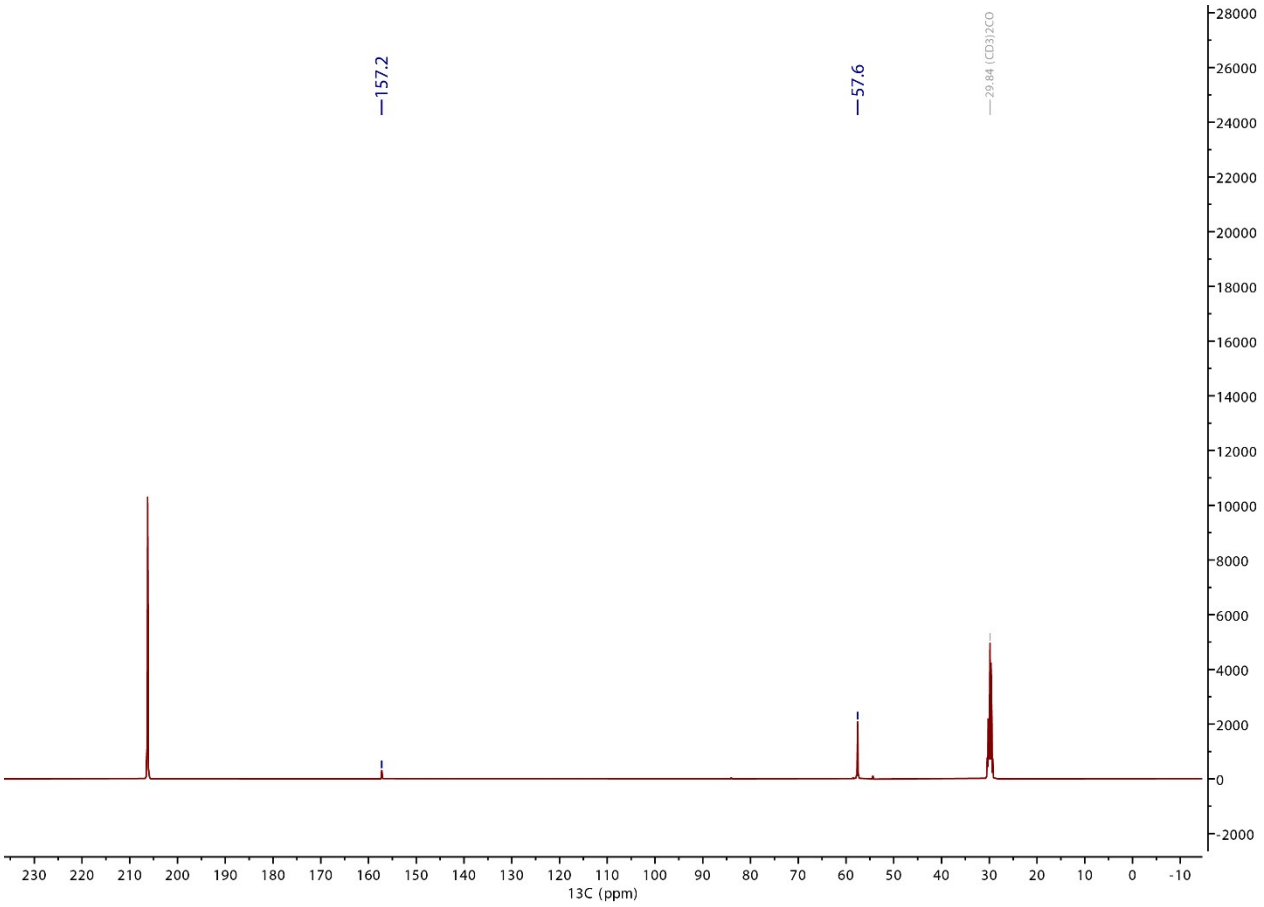

Figure S5. $^{13}C\{^{1}H\}$ NMR of **2** in acetone-d_6.

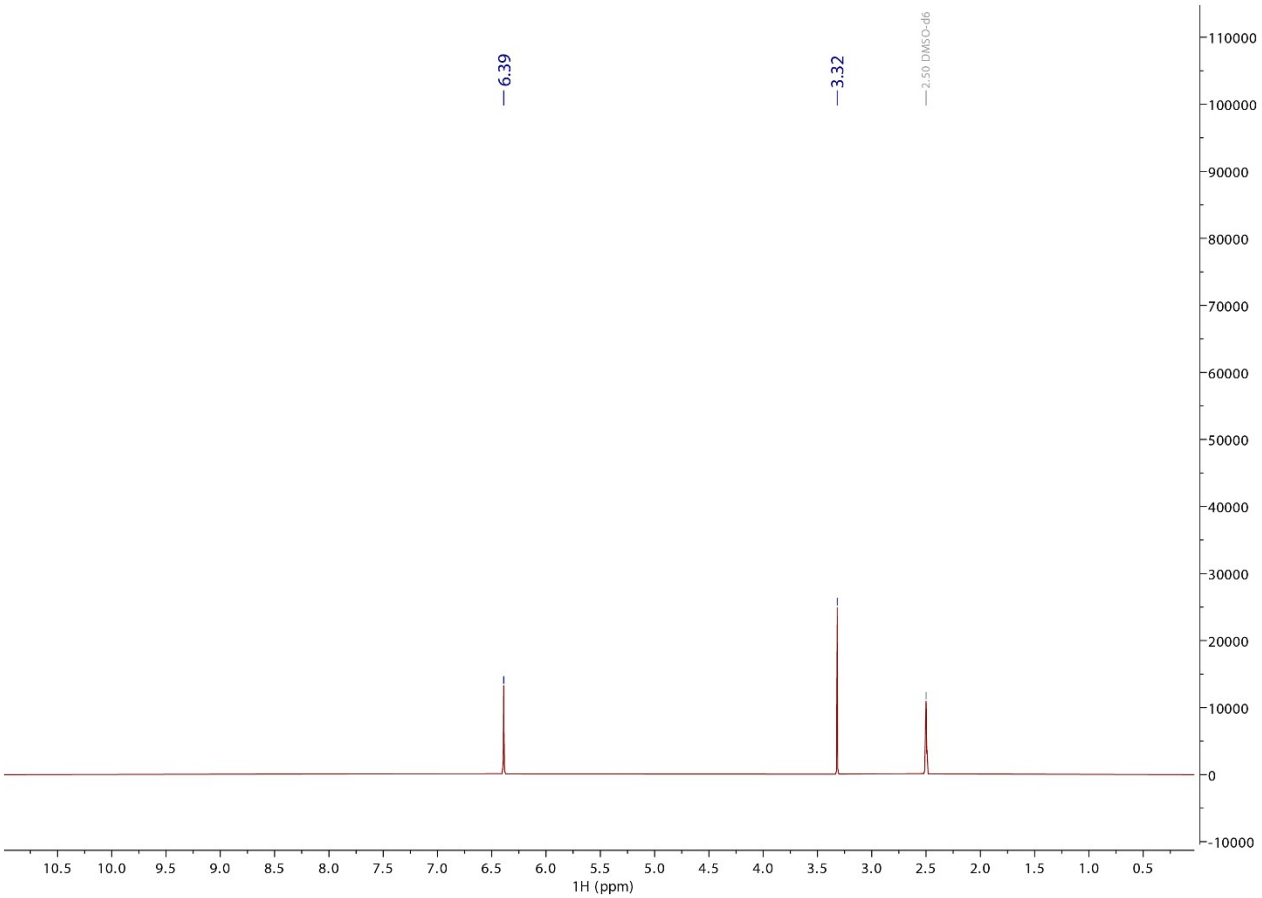

Figure S6. ^{1}H NMR of **3** in DMSO-d_6; residual water at δ = 3.32 ppm.

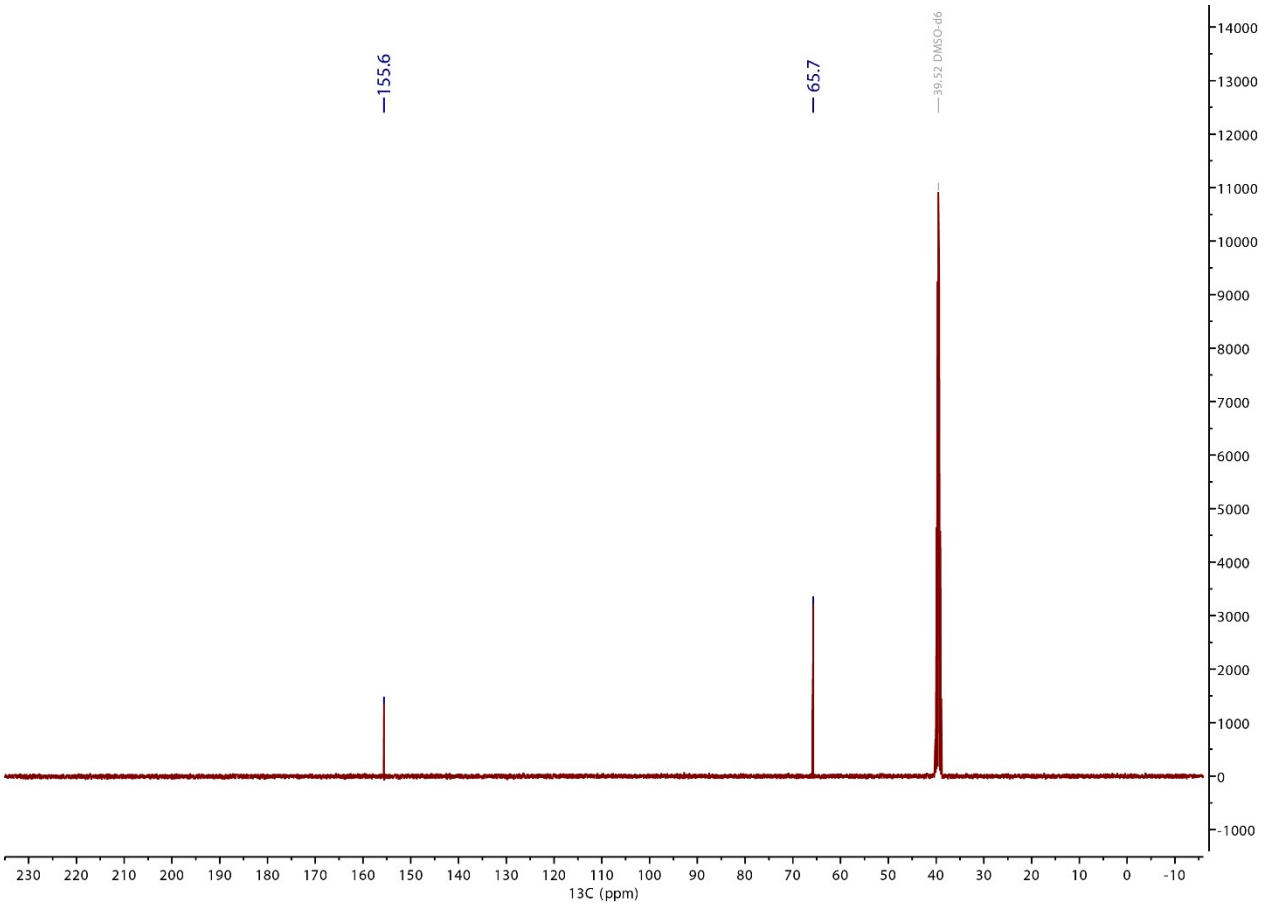

Figure S7. ^{13}C NMR of **3** in DMSO-d_6.

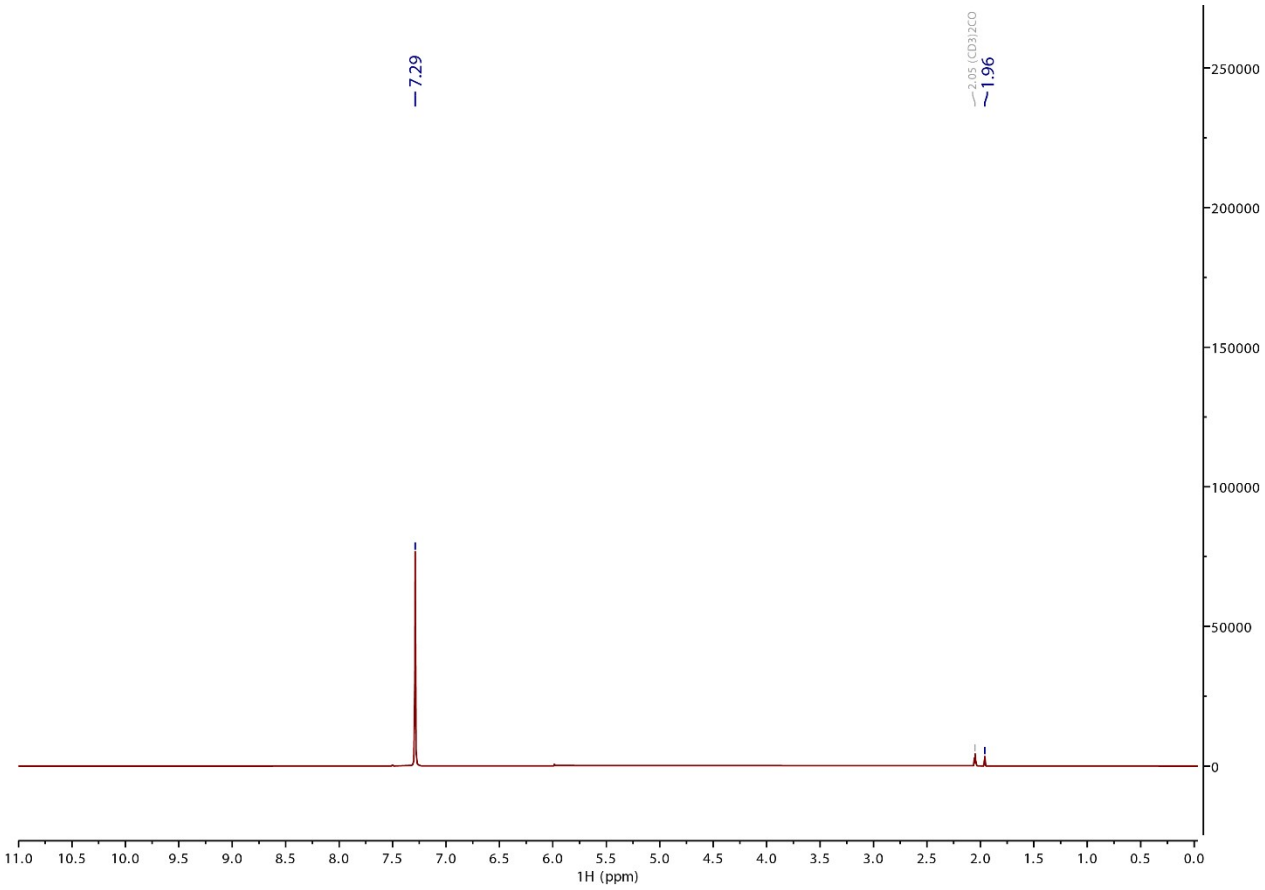

Figure S8. ^{1}H NMR of **4** in acetone-d_6; residual acetone at δ = 1.96 ppm.

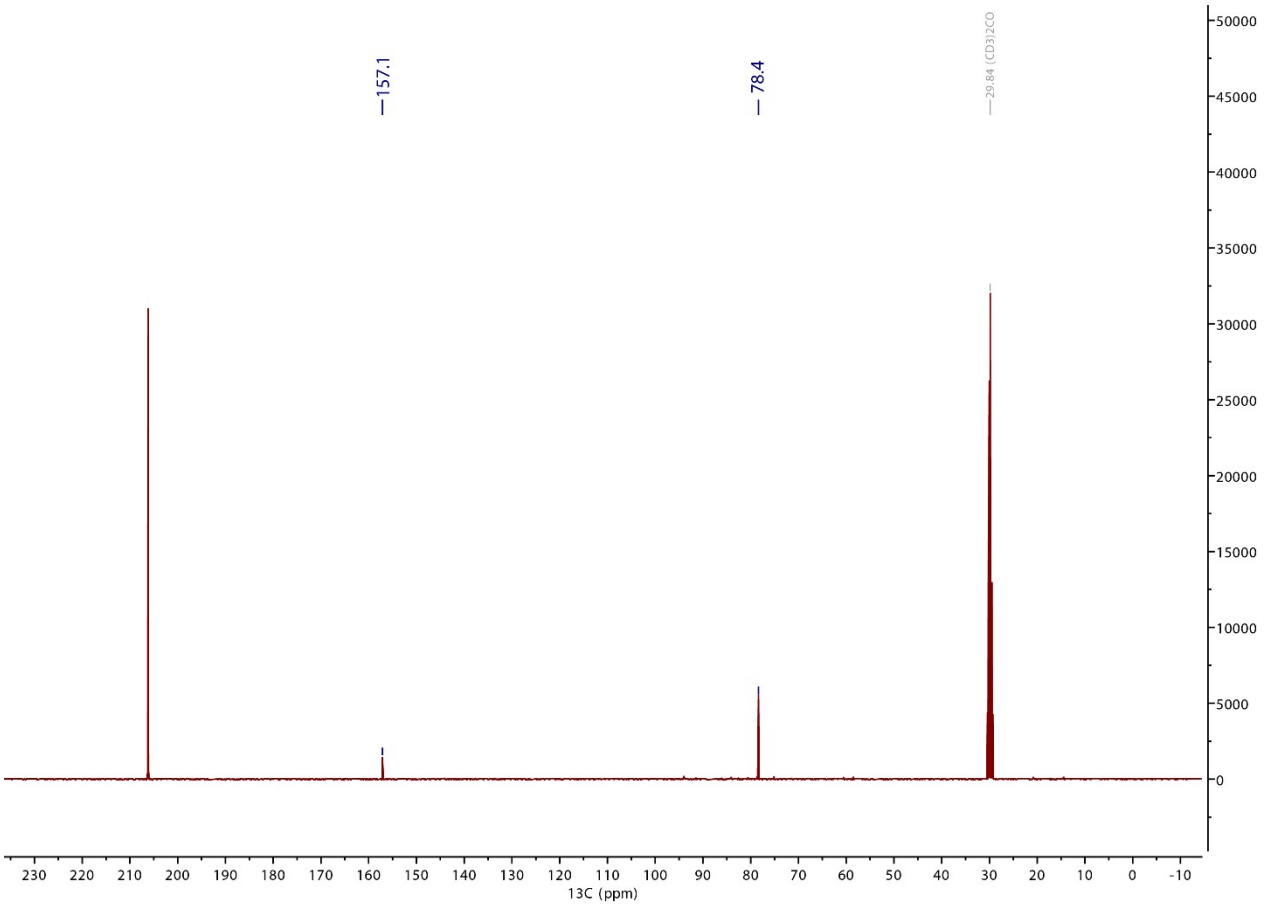

Figure S9. $^{13}C\{^{1}H\}$ NMR of **4** in acetone-d_6.

.

5. IR Spectroscopy

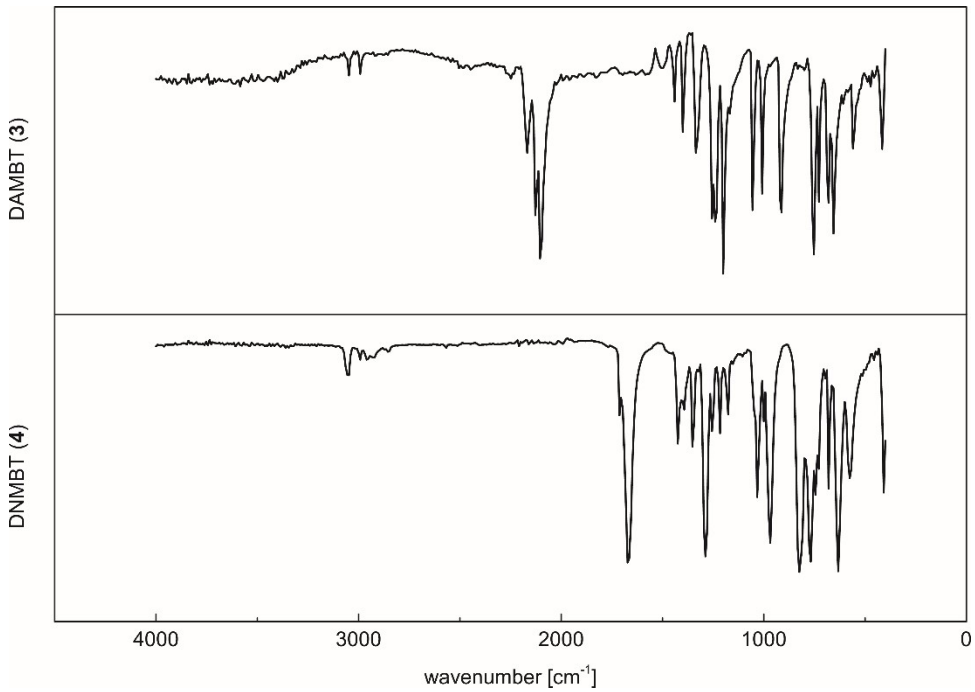

Figure S10. IR spectra of compounds **3** and **4**.

6. DTA measurement

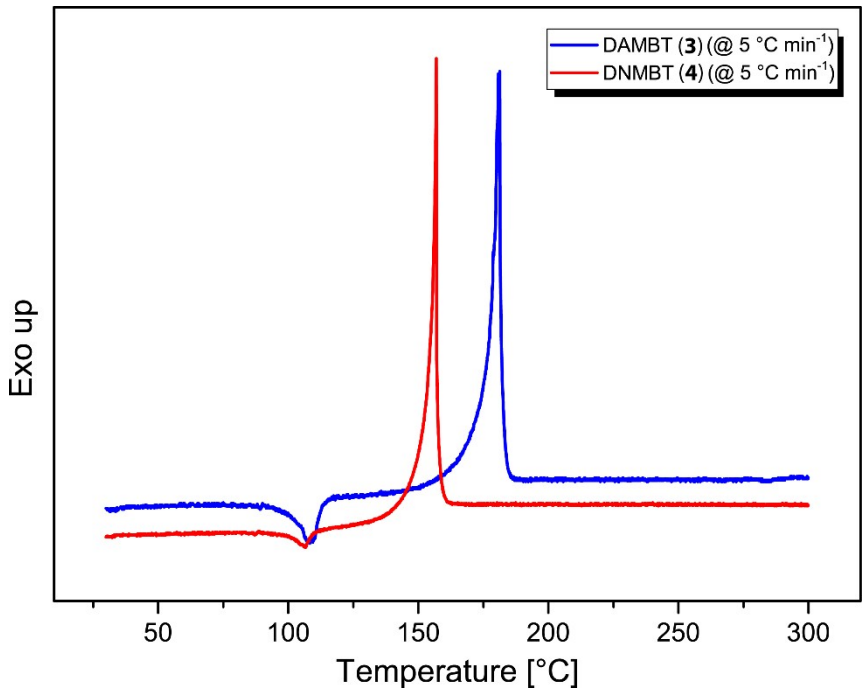

Figure S11. DTA measurement of compounds **3** and **4** with a heating rate of 5 °C min^{-1}.

7. References

S1 NATO standardization agreement (STANAG) on explosives, impact sensitivity tests, no. 4489, 1st ed., Sept. 17, 1999.

S2 WIWEB-Standardarbeitsanweisung 4-5.1.02, Ermittlung der Explosionsgefährlichkeit, hier der Schlagempfindlichkeit mit dem Fallhammer, Nov. 8, 2002.

S3 BAM, http://www.bam.de, (accessed March 2021).

S4 NATO standardization agreement (STANAG) on explosive, friction sensitivity tests, no. 4487, 1st ed., Aug. 22, 2002.

S5 WIWEB-Standardarbeitsanweisung 4-5.1.03, Ermittlung der Explosionsgefährlichkeit oder der Reibeempfindlichkeit mit dem Reibeapparat, Nov. 8, 2002.

S7 OZM, http://www.ozm.cz, (accessed March 2021).

S8 UN Model Regulation: Recommendations on the Transport of Dangerous Goods – Manual of Tests and Criteria, section 13.4.2.3.3, 2015.

S9 Impact: insensitive > 40 J, less sensitive ≥ 35 J, sensitive ≥ 4 J, very sensitive ≤ 3 J; Friction: insensitive > 360 N, less sensitive = 360 N, sensitive < 360 N and > 80 N, very sensitive ≤ 80 N, extremely sensitive ≤ 10 N. According to the UN Recommendations on the Transport of Dangerous Goods, 5th ed., 2009.

S10 M. Sućeska, EXPLO5 Version 6.05 User's Guide. Zagreb, Croatia: OZM; 2018.

S11 M. J. Frisch, G. W. Trucks, H. B. Schlegel, G. E. Scuseria, M. A. Robb, J. R. Cheeseman, G. Scalmani, V.Barone, B. Mennucci, G. A. Petersson, H. Nakatsuji, M. Caricato, X. Li, H.P. Hratchian, A. F. Izmaylov, J. Bloino, G. Zheng, J. L. Sonnenberg, M. Hada, M. Ehara, K. Toyota, R. Fukuda, J. Hasegawa, M. Ishida, T. Nakajima, Y. Honda, O. Kitao, H. Nakai, T. Vreven, J. A. Montgomery, Jr., J. E. Peralta, F. Ogliaro, M. Bearpark, J. J. Heyd, E. Brothers, K. N. Kudin, V. N. Staroverov, R. Kobayashi, J. Normand, K. Raghavachari, A. Rendell, J. C. Burant, S. S. Iyengar, J. Tomasi, M. Cossi, N. Rega, J. M. Millam, M.Klene, J. E. Knox, J. B. Cross, V. Bakken, C. Adamo, J. Jaramillo, R. Gomperts, R. E. Stratmann, O. Yazyev, A. J. Austin, R. Cammi, C. Pomelli, J. W. Ochterski, R. L. Martin, K. Morokuma, V. G. Zakrzewski, G. A. Voth, P. Salvador, J. J. Dannenberg, S. Dapprich, A. D. Daniels, O. Farkas, J.B. Foresman, J. V. Ortiz, J. Cioslowski and D. J. Fox, Gaussian 09 A.02, Gaussian, Inc., Wallingford, CT, USA, 2009.

S12 J. W. Ochterski, G. A. Petersson, J. A. Montgomery Jr., *J. Chem. Phys.* **1996**, *104*, 2598.

S13 CrysAlisPRO (Version 171.33.41), Oxford Diffraction Ltd., 2009.

S14 A. Altomare, G. Cascarano, C. Giacovazzo, and A. Guagliardi, *J. Appl. Crystallogr.*, 1992, **26**, 343.

S15 A. Altomare, G. Cascarano, C. Giacovazzo, A. Guagliardi, A. G. G. Moliterni, M. C. Burla, G. Polidori, M. Camalli and R. Spagna, SIR97, 2003.

S16 A. Altomare, M. C. Burla, M. Camalli, G. L. Cascarano, C. Giacovazzo, A. Guagliardi, A. G. G. Moliterni, G. Polidori and R. Spagna, *J. Appl. Crystallogr.*, 1999, **32**, 115.

S17 G. M. Sheldrick, SHELXL-97, University of Göttingen, Germany, 1997.

S18 G. M. Sheldrick, *Acta Crystallogr. Sect. A*, 2008, **64**, 112.

S19 G. M. Sheldrick, *Acta Cryst. A*, 2015, **71**, 3–8.

S20 A. L. Spek, PLATON, Utrecht University, The Netherlands, 1999.

S21 L.J. Farrugia, *J. Appl. Cryst.*, 2012, **45**, 849.

S22 Empirical absorption correction using spherical harmonics, implemented in SCALE3 ABSPACK scaling algorithm (CrysAlisPro Oxford Diffraction Ltd., Version 171.33.41, 2009).

S23 APEX3, Bruker AXS Inc., Madison, Wisconsin, USA.

S24 J. A. Montgomery Jr., M. J. Frisch, J. W. Ochterski and G. A. Petersson, *J. Chem. Phys.*, 2000, **112**, 6532–6542.

S25 L. A. Curtiss, K. Raghavachari, P. C. Redfern and J. A. Pople, *J. Chem. Phys.*, 1997, **106**, 1063–1079.

S26 E. F. C. Byrd and B. M. Rice, *J. Phys. Chem. A*, 2006, **110**, 1005–1013.

S27 B. M. Rice, S. V. Pai and J. Hare, *Comb. Flame*, 1999, **118**, 445–458.

S28 P. J. Lindstrom and W. G. Mallard, NIST Standard Reference Database Number 69, http://webbook.nist.gov/chemistry/, (accessed March 2021).

S29 M. S. Westwell, M. S. Searle, D. J. Wales and D. H. Williams, *J. Am. Chem. Soc*. 1995, **117**, 5013–5015.

S30 F. Trouton, *Philos. Mag.* 1884, **18**, 54–57.

S31 Equation for volumetric expansion: $\rho_{298K} = \frac{\rho_T}{1 + \alpha_V(298 - T)}$; $\alpha_V = 1.5 \times 10^{-4} K^{-1}$